Correlation between the halo concentration c and the virial mass M_{vir} determined from X-ray clusters

Xiang-Ping Wu and Yan-Jie Xue

Beijing Astronomical Observatory, Chinese Academy of Sciences, Beijing 100012; and

National Astronomical Observatories, Chinese Academy of Sciences, Beijing 100012; China

Received October 4 1999; accepted November 17 1999

ABSTRACT

Numerical simulations of structure formation have suggested that there exists a good correlation between the halo concentration c (or the characteristic density δ_c) and the virial mass M_{vir} for any virialized dark halo described by the Navarro, Frenk & White (1995) density profile. In this *Letter*, we present an observational determination of the c–M_{vir} (or δ_c–M_{vir}) relation in the mass range of $\sim 10^{14}M_\odot < M_{vir} <\sim 10^{16}M_\odot$ using a sample of 63 X-ray luminous clusters. The best-fit power law relation, which is roughly independent of the values of Ω_M and Ω_Λ, is $c \propto M_{vir}^{-0.5}$ or $\delta_c \propto M_{vir}^{-1.2}$, indicating $n \approx -0.7$ for a scale-free power spectrum of the primordial density fluctuations. We discuss the possible reasons for the conflict with the predictions by typical CDM models such as SCDM, LCDM and OCDM.

Subject headings: cosmology: theory — galaxies: clusters: general — X-rays: galaxies

1. Introduction

High-resolution simulations of structure formation have suggested that the virialized dark matter halos with masses spanning several orders of magnitude should follow a universal density profile (Navarro, Frenk & White 1995; NFW)

$$\rho(r) = \frac{\rho_s}{(r/r_s)(1+r/r_s)^2}, \tag{1}$$

where ρ_s and r_s are the characteristic density and length, respectively. The former is further related to the characteristic density δ_c and the critical density $\rho_c = (3H_0^2/8\pi G)Z(z)$ of the Universe at redshift z through $\rho_s = \delta_c\rho_c$, in which $Z(z) = (1+z)^3(\Omega_M/\Omega_M(z))$, and Ω_M is the cosmic density parameter. Although the NFW profile was first obtained in the SCDM model, subsequent numerical studies have shown that this density profile is independent of mass, initial density fluctuation or cosmology (e.g. Cole & Lacey 1996; Navarro, Frenk & White 1997; Eke, Navarro & Frenk 1998; Jing 1999; etc.). The two free parameters in NFW profile can be determined from the halo concentration $c = r_{vir}/r_s$ and the virial mass M_{vir} if the overdensity of the dark matter with respect to the average value is Δ_c,

$$\delta_c = \frac{\Delta_c}{3}\frac{c^3}{\ln(1+c) - c/(1+c)}; \tag{2}$$

$$r_s = \frac{1.626\times 10^{-5}}{c}\left(\frac{M_{vir}}{M_\odot}\right)^{1/3}\left(\frac{\Delta_c}{200}\right)^{-1/3}\left(\frac{1}{Z}\right)^{1/3} h^{-2/3}\ \mathrm{Mpc}. \tag{3}$$

It has been well established based on numerical simulations that there exists a good correlation between the halo concentration c (or the characteristic density δ_c) and the virial mass M_{vir} for any particular cosmology (e.g. Navarro, Frenk & White 1996, 1997; Salvador-Solé, Solanes & Manrique 1998; etc.). For example, given $\Delta_c = 200$, in the mass range of $3\times 10^{11}M_\odot \leq M_{vir} \leq 3\times 10^{15}M_\odot$, the c-M_{vir} relation can be well fitted by a power-law function: $c = a(M_{vir}/M_\odot)^b$, with $(a,b) = (891, -0.14)$ and $(186, -0.10)$ for SCDM model ($\Omega_M = 1.0$, $\Omega_\Lambda = 0$, $h = 0.5$ and $\sigma_8 = 0.65$) and ΛCDM model ($\Omega_M = 0.25$, $\Omega_\Lambda = 0.75$, $h = 0.75$ and $\sigma_8 = 1.3$), respectively. While the NFW profile and the c-M_{vir}

correlation are only determined from simulations for halo masses as small as $M_{vir} = 10^{11} M_{\odot}$ or as large as $M_{vir} = 10^{15} M_{\odot}$, there is no reason to believe that these results would not be valid for halos which are one order of magnitude lower or higher in mass (Burkert & Silk 1999).

On the other hand, observationally we can only measure the distribution of baryonic matter rather than that of dark halo. It is crucial to link numerical predictions with astronomical observations. In a fully virialized system, the distribution and motion of baryonic matter can be determined by the underlying gravitational potential of the dark halo, if the velocity dispersion or temperature profile can be well measured. It is thus possible to work out the dynamical properties of the dark matter halo such as M_{vir}, r_s, r_{vir}, c or δ_c from the observed distribution of luminous matter in a gravitationally bound system. This will eventually allow us to examine observationally whether there is a correlation between c (or δ_c) and M_{vir}. Finally, a comparison of the observationally determined and numerically simulated c–M_{vir} (or δ_c–M_{vir}) correlations may provide a useful way to distinguish different cosmological models. In this *Letter*, we will make an attempt for the first time to derive the c–M_{vir} and δ_c–M_{vir} correlations on cluster scales by fitting the observed X-ray surface brightness profiles of clusters to those predicted by the NFW profile as the cluster dark halos under the assumption of isothermality. Note that there is a striking similarity between the distribution of intracluster gas tracing the dark halo of the NFW potential and the conventional β model. Makino, Sasaki & Suto (1998) have explicitly shown that the NFW profile via isothermal hydrostatic equilibrium results in an analytic form of gas distribution

$$n_{gas}(r) = n_{gas}(0) e^{-\alpha} (1 + r/r_s)^{\alpha/(r/r_s)}, \tag{4}$$

in which $\alpha = 4\pi G \mu m_p \rho_s r_s^2 / kT$, and $\mu = 0.585$ denotes the mean molecular weight. Briefly, our task is to determine the best-fit parameters of α and r_s for an ensemble of X-ray

clusters in terms of eq.(4), and then derive the relevant parameters ρ_s and δ_c in conjunction with the X-ray temperature T. Finally, we examine the c-M_{vir} and δ_c–M_{vir} correlations by solving eqs.(2) and (3).

2. Sample

Essentially, we select our cluster sample from two ROSAT PSPC cluster catalogs: the 36 high-luminosity clusters by Ettori & Fabian (1999; EF) and the 45 nearby clusters by Mohr, Mathiesen & Evrard (1999; MME). The EF clusters have high X-ray luminosity $L_x > 10^{45}$ erg s^{-1}, and a great fraction of them also have relatively high redshift $z \approx 0.1$–0.3. The best-fit values of α and r_s for all the 36 EF clusters have been given by EF for a cosmological model of $H_0 = 50$ km s^{-1} Mpc^{-1} and $\Omega_M = 1$. A conversion of r_s into the values in different cosmological models should be properly made, if needed. The MME clusters are taken from an X-ray flux limited sample, and thereby located at relatively small redshift. We perform the χ^2 fit of the observed X-ray surface brightness profiles of the MME clusters to the theoretical prediction $S_x \propto \int n_{gas}^2 d\ell$ according to thermal bremsstrahlung, where the integral is made along the line of sight. A cross-identification reveals that 16 clusters are listed in both samples, for which our fitted values of α and r_s are fairly consistent with those obtained by EF. We further require that the X-ray temperature should be observationally available, and we take the temperature data from Wu, Xue & Fang (1999; and references therein). The finally merged EF and MME sample to be used in our following analysis contains 63 clusters.

3. The c-M_{vir} and δ_c-M_{vir} correlations

We confine ourselves to a flat cosmological model with $\Omega_M + \Omega_\Lambda = 1$. In this case, the density contrast depends on the value of Ω_M and can be approximated by (Eke et al. 1998) $\Delta_c = 178\Omega_M(z)^{0.45}$, and $Z(z) = (1+z)^2\{1 + z\Omega_M + [(1+z)^{-2} - 1]\Omega_\Lambda\}$ and $\Omega_M(z) = \Omega_M(1+z)^3/Z(z)$. For a given cosmological model $(\Omega_M, \Omega_\Lambda)$, we convert our best-fit values of α and r_s into δ_c and then obtain the concentration parameter c and the virial mass M_{vir} by numerically solving eqs.(2) and (3). We display in Fig.1 an example of the resultant c and δ_c versus M_{vir} for $\Omega_M = 0.3$ and $\Omega_\Lambda = 0.7$. It is apparent that there exists a strong correlation between c or δ_c and M_{vir}. We employ the Monte-Carlo simulations and the χ^2 fitting method to obtain the best-fit c-M_{vir} and δ_c-M_{vir} relations which are assumed to be a power-law. This enables us to include the measurement uncertainties in both axes. Note that for the EF clusters we have not accounted for the uncertainties arising from the fitted parameters of α and r_s since EF provided no information about their error estimates. The results for a set of cosmological models are listed in Table 1. Additionally, we have tried the orthogonal distance regression technique ODRPACK (e.g. Feigelson & Babu 1992) and reached a steeper power index. For example, in the case of $\Omega_M = 0.3$ and $\Omega_\Lambda = 0.7$ we find $c = 10^{14.47\pm1.03}(M_{vir}/M_\odot)^{-0.92\pm0.07}$ and $\delta_c = 10^{33.15\pm2.28}(M_{vir}/M_\odot)^{-1.97\pm0.15}$ (see Fig.1). Although ODRPACK can simultaneously account for the scatters around M_{vir} and c (or δ_c), the goodness of the fit has not been improved for our problem in the sense that the reduced χ^2 for both c-M_{vir} and δ_c-M_{vir} relations are significantly larger than those obtained using the χ^2 fitting method along with Monte-Carlo simulations. In Table 1 we have also given the power index for a scale-free power spectrum of initial density fluctuations implied by our best-fit δ_c-M_{vir} relation: $\delta_c \propto M_{vir}^{-(n+3)/2}$ (NFW), which yields $n \approx -0.7$.

EDITOR: PLACE FIGURE 1 HERE.

4. Discussion and conclusions

In a virialized system, the distribution and motion of galaxies and intracluster gas (if their self-gravity is negligible) are determined by the underlying gravitational potential of the dark matter halo, provided that the velocity dispersion and temperature profiles are well measured. Therefore, one can probe the dynamical properties of the dark matter halo, though it is invisible, by using optical/X-ray observations coupled with the hydrostatic equilibrium hypothesis. In this *Letter*, we have made an attempt to derive the halo concentration c, the characteristic density δ_c and the virial mass M_{vir} for galaxy clusters characterized by the NFW profile from the observed distribution and temperature of X-ray emitting gas. Although the correlation between c (or δ_c) and M_{vir} has been well predicted from numerical simulations, this is the first time to determine the c–M_{vir} and δ_c–M_{vir} correlations making use of the real data from astronomical observations.

The correlation between c (or δ_c) and M_{vir} established in this *Letter* is applicable to massive halos in the mass range of $\sim 10^{14}M_{\odot} < M_{vir} <\sim 10^{16}M_{\odot}$. However, we notice that the resultant slope (≈ -0.5) of the $\log c$–$\log M_{vir}$ relationship is significantly steeper while the spectrum ($n \approx -0.7 \pm 0.3$) of the primordial density fluctuations is much flatter than the values predicted by typical CDM spectra for the mass halos with $3 \times 10^{11}M_{\odot} < M_{vir} < 3 \times 10^{15}M_{\odot}$ (Burkert & Silk 1999), especially on cluster scales where $n \approx -2$ (e.g. Henry & Arnaud 1991; Mathiesen & Evrard 1998; Donahue & Voit 1999; Mahdavi 1999; etc.). If our results are not a statistical fluke (Note the large dispersion of the X-ray data points in Fig.1), the above conflict may imply that we should abandon at least one of our working hypotheses: (1)Intracluster gas is in hydrostatic equilibrium; (2)Intracluster gas has isothermal temperature profile; (3)The self-gravity of intracluster gas is considerably small as compared with the contribution of the dark matter halo; (4)The NFW profile provides a precise description of the dark matter distribution. Yet,

further investigations should be made towards a robust constraint on the c–M_{vir} and δ_c–M_{vir} relations before we come to a detailed study of the possible reasons for the reported discrepancy.

We note from Table 1 that our best-fit c–M_{vir} and δ_c–M_{vir} relations and the constraints on n are roughly independent of the cosmological models (Ω_m and Ω_Λ). This property will be significant for distinguishing different cosmological models when combined with high-resolution numerical simulations.

We gratefully acknowledge the valuable comments by an anonymous referee. This work was supported by the National Science Foundation of China, under Grant No. 19725311.

Table 1. The best-fit c-M_{vir} and δ_c-M_{vir} relations

Ω_M	Ω_Λ	c-M_{vir} correlation	δ_c-M_{vir} correlation	n
0.15	0.85	$c = 10^{8.17\pm0.58}(M_{vir}/M_\odot)^{-0.50\pm0.04}$	$\delta_c = 10^{20.77\pm1.54}(M_{vir}/M_\odot)^{-1.14\pm0.10}$	-0.72 ± 0.20
0.30	0.70	$c = 10^{8.23\pm0.63}(M_{vir}/M_\odot)^{-0.51\pm0.04}$	$\delta_c = 10^{20.83\pm1.64}(M_{vir}/M_\odot)^{-1.15\pm0.11}$	-0.70 ± 0.22
0.50	0.50	$c = 10^{8.29\pm0.69}(M_{vir}/M_\odot)^{-0.51\pm0.05}$	$\delta_c = 10^{20.89\pm1.76}(M_{vir}/M_\odot)^{-1.16\pm0.12}$	-0.68 ± 0.24
0.70	0.30	$c = 10^{8.32\pm0.74}(M_{vir}/M_\odot)^{-0.52\pm0.05}$	$\delta_c = 10^{20.92\pm1.86}(M_{vir}/M_\odot)^{-1.16\pm0.13}$	-0.68 ± 0.26
1.00	0.00	$c = 10^{8.35\pm0.81}(M_{vir}/M_\odot)^{-0.53\pm0.06}$	$\delta_c = 10^{20.93\pm1.99}(M_{vir}/M_\odot)^{-1.17\pm0.14}$	-0.66 ± 0.28

REFERENCES

Burkert, A., & Silk, J., 1999, preprint astro-ph/9904159

Cole, S., & Lacey, C., 1996, MNRAS, 281, 716

Ettori, S., & Fabian, A. C., 1999, MNRAS, 305, 834 (EF)

Eke, V. R., Navarro, J. F., & Frenk, C. S., 1998, ApJ, 503, 569

Donahue, M., & Voit, G. M., 1999, ApJ, in press (astro-ph/9907333)

Feigelson, E. D., & Babu, G. J., 1992, ApJ, 397, 55

Henry, J. P., & Arnaud, K. A., 1991, ApJ, 372, 410

Jing, Y.-P., 1999, ApJ, submitted (astro-ph/9901340)

Mahdavi, A., 1999, ApJ, in press (astro-ph/9905270)

Makino, N., Sasaki, S., & Suto, Y., 1998, ApJ, 497, 555

Mathiesen, B., & Evrard, A. E., 1998, MNRAS, 295, 769

Mohr, J. J., Mathiesen, B., & Evrard, A. E., 1999, ApJ, 517, 627 (MME)

Navarro, J. F., Frenk, C. S., & White, S. D. M., 1995, MNRAS, 275, 720 (NFW)

Navarro, J. F., Frenk, C. S., & White, S. D. M., 1996, ApJ, 426, 563

Navarro, J. F., Frenk, C. S., & White, S. D. M., 1997, ApJ, 490, 493

Salvador-Solé, E., Solanes, J. M., & Manrique, A., 1998, ApJ, 499, 542

Wu, X.-P., Xue, Y.-J., & Fang, L.-Z. 1999, ApJ, 524, 22

This manuscript was prepared with the AAS LaTeX macros v4.0.

Table 2. Cluster sample*

cluster	z	T (keV)	α	r_s (Mpc)
A85	0.0559	$6.20^{+0.40}_{-0.50}$	$8.465^{+0.116}_{-0.116}$	$0.360^{+0.021}_{-0.021}$
A119	0.0443	$5.59^{+0.27}_{-0.27}$	$12.30^{+1.078}_{-1.078}$	$2.585^{+0.355}_{-0.355}$
A262	0.0169	$2.41^{+0.05}_{-0.05}$	$6.718^{+0.113}_{-0.113}$	$0.094^{+0.008}_{-0.008}$
A401	0.0737	$8.00^{+0.40}_{-0.40}$	$8.867^{+0.092}_{-0.092}$	$0.930^{+0.027}_{-0.027}$
A426	0.0179	$6.79^{+0.12}_{-0.12}$	$8.084^{+0.108}_{-0.108}$	$0.181^{+0.012}_{-0.012}$
A478	0.0881	$6.90^{+0.35}_{-0.35}$	$9.507^{+0.107}_{-0.107}$	$0.419^{+0.018}_{-0.018}$
A496	0.0325	$4.13^{+0.08}_{-0.08}$	$8.001^{+0.118}_{-0.118}$	$0.195^{+0.014}_{-0.014}$
A520	0.2010	$8.59^{+0.93}_{-0.93}$	$11.35^{+0.0}_{-0.0}$	$1.70^{+0.0}_{-0.0}$
A545	0.1530	$5.50^{+6.20}_{-1.10}$	$12.52^{+0.0}_{-0.0}$	$1.51^{+0.0}_{-0.0}$
A586	0.1710	$6.61^{+1.15}_{-0.96}$	$8.81^{+0.0}_{-0.0}$	$0.26^{+0.0}_{-0.0}$
A644	0.0704	$6.59^{+0.17}_{-0.17}$	$8.771^{+0.158}_{-0.158}$	$1.175^{+0.051}_{-0.051}$
A665	0.1816	$8.26^{+0.90}_{-0.90}$	$10.69^{+0.0}_{-0.0}$	$1.49^{+0.0}_{-0.0}$
A754	0.0535	$9.00^{+0.50}_{-0.50}$	$10.33^{+0.373}_{-0.373}$	$0.774^{+0.066}_{-0.066}$
A780	0.0552	$3.57^{+0.10}_{-0.10}$	$9.441^{+0.372}_{-0.372}$	$0.285^{+0.046}_{-0.046}$
A1060	0.0126	$3.24^{+0.06}_{-0.06}$	$8.543^{+0.199}_{-0.199}$	$0.314^{+0.018}_{-0.018}$
A1068	0.1390	$5.50^{+0.90}_{-0.90}$	$9.72^{+0.0}_{-0.0}$	$0.42^{+0.0}_{-0.0}$
A1367	0.0214	$3.50^{+0.18}_{-0.18}$	$10.88^{+0.696}_{-0.696}$	$1.863^{+0.179}_{-0.179}$
A1413	0.1427	$8.85^{+0.50}_{-0.50}$	$9.17^{+0.0}_{0.0}$	$0.57^{+0.0}_{-0.0}$
A1651	0.0825	$6.10^{+0.20}_{-0.20}$	$9.082^{+0.191}_{-0.563}$	$0.563^{+0.033}_{-0.033}$
A1656	0.0231	$8.38^{+0.34}_{-0.34}$	$22.36^{+2.167}_{-2.167}$	$3.471^{+0.414}_{-0.414}$
A1689	0.1810	$9.02^{+0.40}_{-0.40}$	$10.93^{+0.443}_{-0.443}$	$0.715^{+0.074}_{-0.074}$
A1763	0.1870	$8.98^{+1.02}_{-0.84}$	$9.20^{+0.0}_{-0.0}$	$1.16^{+0.0}_{-0.0}$
A1795	0.0631	$5.88^{+0.14}_{-0.14}$	$10.04^{+0.148}_{-0.148}$	$0.462^{+0.025}_{-0.025}$
A1835	0.2523	$9.80^{+1.40}_{-1.40}$	$10.22^{+0.0}_{-0.0}$	$0.32^{+0.0}_{-0.0}$
A2029	0.0765	$8.47^{+0.41}_{-0.36}$	$9.198^{+0.133}_{-0.133}$	$0.390^{+0.022}_{-0.022}$
A2052	0.0348	$3.10^{+0.20}_{-0.20}$	$8.358^{+0.149}_{-0.149}$	$0.204^{+0.014}_{-0.014}$
A2063	0.0355	$3.68^{+0.11}_{-0.11}$	$8.194^{+0.149}_{-0.149}$	$0.362^{+0.020}_{-0.020}$
A2142	0.0899	$9.70^{+1.30}_{-1.30}$	$9.446^{+0.357}_{-0.357}$	$0.636^{+0.091}_{-0.091}$
A2163	0.2030	$14.69^{+0.85}_{-0.85}$	$9.16^{+0.0}_{-0.0}$	$1.09^{+0.0}_{-0.0}$
A2199	0.0299	$4.10^{+0.08}_{-0.08}$	$9.131^{+0.081}_{-0.081}$	$0.315^{+0.012}_{-0.012}$
A2204	0.1523	$9.20^{+1.50}_{-1.50}$	$8.633^{+0.122}_{-0.122}$	$0.236^{+0.018}_{-0.018}$
A2218	0.1710	$7.10^{+0.20}_{-0.20}$	$10.32^{+0.0}_{-0.0}$	$0.99^{+0.0}_{-0.0}$
A2219	0.2280	$12.40^{+0.50}_{-0.50}$	$11.51^{+0.0}_{-0.0}$	$1.59^{+0.0}_{-0.0}$
A2244	0.0970	$8.47^{+0.43}_{-0.42}$	$8.033^{+0.223}_{-0.223}$	$0.356^{+0.037}_{-0.037}$
A2255	0.0808	$7.30^{+1.10}_{-1.70}$	$24.80^{+6.635}_{-6.635}$	$5.991^{+1.982}_{-1.982}$

Table 2—Continued

cluster	z	T (keV)	α	r_s (Mpc)
A2256	0.0581	$7.51^{+0.19}_{-0.19}$	$13.21^{+0.655}_{-0.655}$	$2.026^{+0.180}_{-0.180}$
A2319	0.0559	$9.12^{+0.15}_{-0.15}$	$8.306^{+0.143}_{-0.143}$	$0.831^{+0.041}_{-0.041}$
A2390	0.2279	$11.10^{+1.00}_{-1.00}$	$9.25^{+0.0}_{-0.0}$	$0.64^{+0.0}_{-0.0}$
A2507	0.1960	$9.40^{+1.60}_{-1.20}$	$12.53^{+0.0}_{-0.0}$	$2.63^{+0.0}_{-0.0}$
A2597	0.0852	$4.40^{+0.40}_{-0.70}$	$6.236^{+0.783}_{-0.783}$	$0.464^{+0.129}_{-0.129}$
A2744	0.3080	$11.00^{+0.50}_{0.50}$	$15.21^{+0.0}_{-0.0}$	$2.76^{+0.0}_{-0.0}$
A3112	0.0746	$4.24^{+0.24}_{-0.24}$	$8.412^{+0.075}_{-0.075}$	$0.209^{+0.010}_{-0.010}$
A3158	0.0575	$5.50^{+0.30}_{-0.40}$	$10.28^{+0.383}_{-0.383}$	$1.093^{+0.081}_{-0.081}$
A3266	0.0594	$8.00^{+0.30}_{-0.30}$	$14.11^{+0.889}_{-0.889}$	$2.438^{+0.243}_{-0.243}$
A3391	0.0553	$5.40^{+0.60}_{-0.60}$	$7.203^{+0.297}_{-0.297}$	$0.579^{+0.065}_{-0.065}$
A3526	0.0114	$3.68^{+0.06}_{-0.06}$	$6.985^{+0.094}_{-0.094}$	$0.057^{+0.004}_{-0.004}$
A3532	0.0559	$4.40^{+4.70}_{-1.30}$	$9.146^{+0.380}_{-0.380}$	$0.934^{+0.079}_{-0.079}$
A3558	0.0475	$5.12^{+0.20}_{-0.20}$	$7.875^{+0.205}_{-0.205}$	$0.579^{+0.040}_{-0.040}$
A3562	0.0478	$3.80^{+0.50}_{-0.50}$	$6.938^{+0.099}_{-0.099}$	$0.378^{+0.022}_{-0.022}$
A3571	0.0396	$6.73^{+0.17}_{-0.17}$	$9.253^{+0.205}_{-0.205}$	$0.659^{+0.040}_{-0.040}$
A3667	0.0566	$7.0^{+0.6}_{-0.6}$	$8.881^{+0.158}_{-0.158}$	$1.175^{+0.051}_{-0.051}$
A4038	0.0302	$3.30^{+1.60}_{-0.80}$	$5.842^{+0.082}_{-0.082}$	$0.047^{+0.004}_{-0.004}$
A4059	0.0478	$3.97^{+0.12}_{-0.12}$	$8.645^{+0.198}_{-0.198}$	$0.332^{+0.023}_{-0.023}$
AWM7	0.0176	$3.75^{+0.09}_{-0.09}$	$8.756^{+0.194}_{-0.194}$	$0.357^{+0.024}_{-0.024}$
Cygnus-A	0.0570	$6.50^{+0.36}_{-0.36}$	$7.151^{+0.071}_{-0.071}$	$0.101^{+0.008}_{-0.008}$
IRAS 09104	0.4420	$8.50^{+3.40}_{-3.40}$	$10.09^{+0.0}_{-0.0}$	$0.18^{+0.0}_{-0.0}$
MKW3s	0.0434	$3.00^{+0.30}_{-0.30}$	$8.422^{+0.129}_{-0.129}$	$0.219^{+0.012}_{-0.012}$
MS1358	0.3283	$7.50^{+4.30}_{-4.30}$	$14.29^{+0.0}_{-0.0}$	$1.48^{+0.0}_{-0.0}$
MS2137	0.3130	$4.37^{+0.38}_{-0.72}$	$11.48^{+0.0}_{-0.0}$	$0.18^{+0.0}_{-0.0}$
Ophia-A	0.0280	$9.10^{+0.30}_{-0.30}$	$9.004^{+0.558}_{-0.558}$	$0.570^{+0.093}_{-0.093}$
PKS 0745-19	0.1028	$8.70^{+1.60}_{-1.20}$	$8.930^{+0.096}_{-0.096}$	$0.270^{+0.014}_{-0.014}$
Tria-A	0.0510	$10.05^{+0.69}_{-0.69}$	$9.277^{+0.088}_{-0.088}$	$1.042^{+0.023}_{-0.023}$
ZW3146	0.2906	$6.35^{+0.37}_{-0.34}$	$10.26^{+0.0}_{-0.0}$	$0.19^{+0.0}_{-0.0}$

*This table is only available in electronic form.

Fig. 1.— The c–M_{vir} and δ_c–M_{vir} relations for 63 clusters in the case of $\Omega_M = 0.3$ and $\Omega_\Lambda = 0.7$. The MME and EF clusters are represented by the filled and open circles, respectively. Note that the error bars for the EF clusters have only accounted for the temperature uncertainties. The solid lines are the best χ^2 fitted power law relations to the data sets, while the dotted lines represent the results using the ODRPACK fitting method.

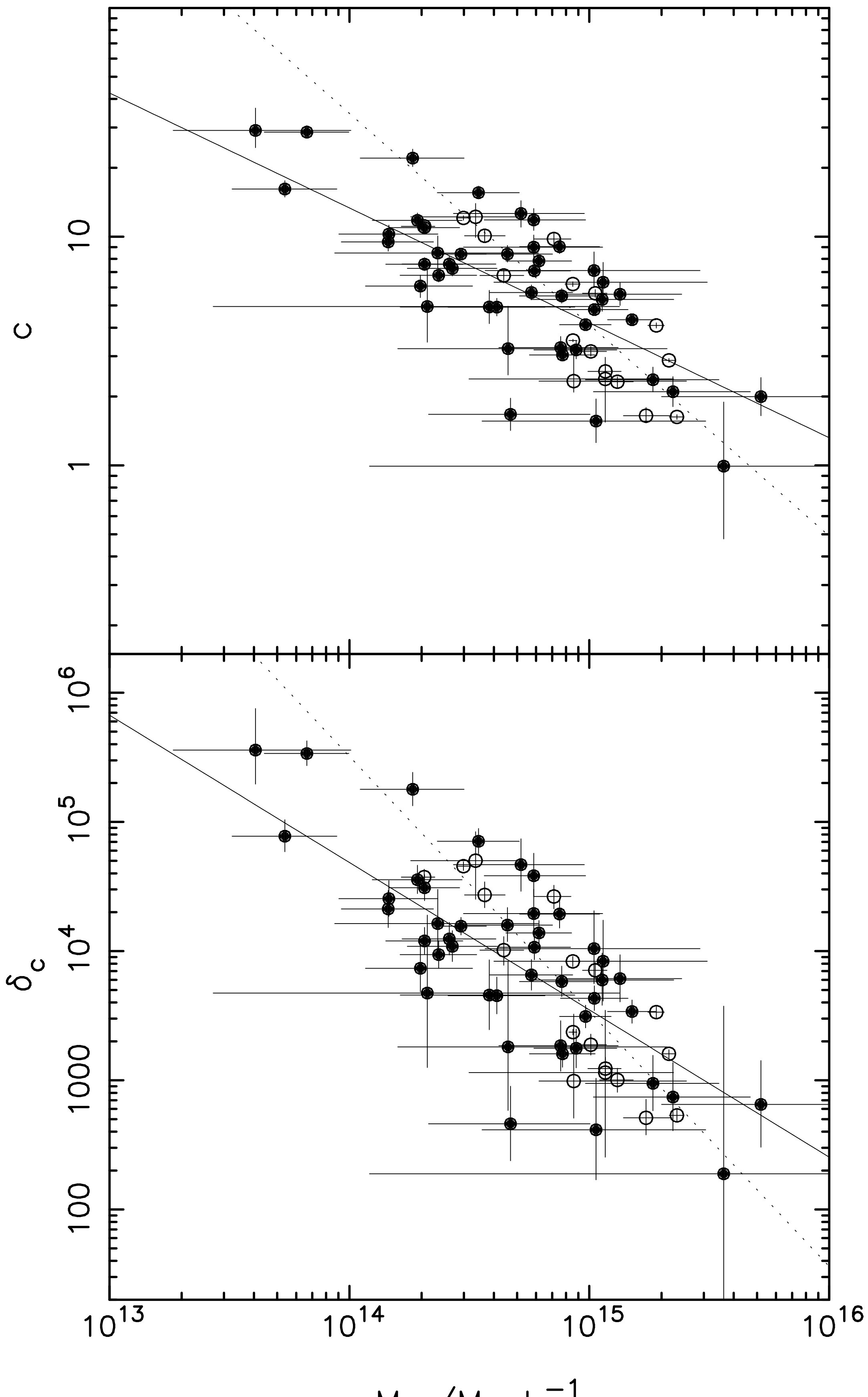
c
10
1
δ_c
10^6
10^5
10^4
1000
100
10^{13}
10^{14}
10^{15}
10^{16}
$M_{vir}/M_\odot\ h^{-1}$